Optimization of ICPCVD Amorphous Silicon for Optical MEMS Applications

Dhirendra Kumar Tripathi, *Member, IEEE*, Fei Jiang, Mariusz Martyniuk, *Member, IEEE*, Jarek Antoszewski, K. K. M. B. Dilusha Silva, *Member, IEEE*, John M. Dell, *Member, IEEE*, and Lorenzo Faraone, *Fellow, IEEE*

***Abstract*— In this paper, we present the optimization of optical and mechanical properties of inductively coupled plasma chemical vapor deposited (ICPCVD) amorphous silicon thin films for fabrication of high-quality optical microelectromechanical systems-based devices operating from visible to short-wave infrared wavelengths (450–3000 nm). Our results indicate that, at relatively high deposition temperatures for plasma CVD, a decrease in the ICP power results in films with lower tensile stress, higher refractive index, and lower extinction coefficient. We show that hydrogen concentration alone is not a sufficient parameter for controlling optical and mechanical quality of the films. In particular, both the hydrogen concentration and the hydrogen-silicon bonding nature together play a vital role in determining the optical and the mechanical quality of the silicon thin films. As a demonstration vehicle, three layer silicon–silicon oxide–silicon-based distributed Bragg reflectors were fabricated for the visible (500–700 nm), near infrared (700–1000 nm), and short-wave infrared (2000–3000 nm) wavelength ranges using an optimized silicon fabrication recipe. The measured optical transmission spectra show close to 90% peak reflectivity. Finally, stress optimization was evaluated by fabricating 270-μm diameter circular suspended silicon membranes, which demonstrate a flatness variation on the order of <6 nm across the entire lateral dimension. [2015-0029]**

***Index Terms*— Optical microelectromechanical systems (MEMS), distributed Bragg reflector (DBR), optical constants, silicon-hydrogen bonding.**

I. Introduction

A MYRIAD of technological advances have made possible the recent development of field-portable microelectromechanical systems (MEMS) based optical sensing systems. The advantages include system miniaturization, the capacity to be used in harsh environments, and cost effectiveness in comparison to the bench-top FTIR systems. Such optical systems are generally based on MEMS optical filters and reflectors that are now integral components in medical imaging devices, defense and security systems, spectrometers, and telecommunication and display technologies [1]–[3].

An important class of optical MEMS includes tunable Fabry-Perot (FP) filters. These filters are wavelength selective elements constructed from two distributed Bragg reflectors (DBR), one of which is fixed and the other actuated so as to modulate the transmitted wavelength. A simple three-layer DBR consists of two high refractive index dielectric layers separated by a low index dielectric material. Each of the three layers is a quarter wavelength in optical thickness. The DBR layer thicknesses dictate the operational wavelength range of the DBR and also of the corresponding FP filter. The choice of mirror materials dictates the mirror reflectivity and, thereby, the finesse of the FP filter. FP filters typically require high reflectivity mirrors, and the highest reflectivity for a specified value of period (N) is achieved when the first layer has a high refractive index [4], for light incident from free space. For a lossless N-period DBR with a high-index first layer, the mirror reflectivity R at the central design wavelength λ_C is given by [4]

$$R(N) = \left(\frac{1 - n_S \left(n_H/n_L\right)^{2N}}{1 + n_S \left(n_H/n_L\right)^{2N}} \right)^2 \tag{1}$$

where n_S, n_H, n_L represents refractive index of incident medium, high-index material and low-index material, respectively. F, the finesse of the filter, is related with the reflectivity by the following expression:

$$F = \frac{\pi \sqrt{R}}{1 - R} \tag{2}$$

The free spectral range, $\Delta\lambda$ which is the wavelength separation between adjacent transmission peaks, is related with finesse and full width half maximum (FWHM) $\delta\lambda$ of filter with the following expression:

$$F = \frac{\Delta\lambda}{\delta\lambda} \tag{3}$$

As shown in Eq. (1-3) A higher refractive index contrast between the high and low index media in the DBR results in higher DBR reflectivity, higher FP filter finesse and, thus, better spectral resolution. In other words, the requirement of high finesse dictates that we maximize the refractive index of one material and minimize the refractive index of the other. The tuning of distance between the two DBR's determines the optical cavity length, and thus it will decide the wavelength tuning range of the FP filter [4].

Manuscript received January 26, 2015; revised July 8, 2015; accepted July 17, 2015. Date of publication August 5, 2015; date of current version November 25, 2015. This work was supported in part by the Grains Research and Development Corporation, in part by the Australian Research Council Research Grants, and in part by the Western Australian State Government Office of Science. Subject Editor R. Maboudian.

The authors are with the School of Electrical, Electronics, and Computer Engineering, University of Western Australia, Perth, WA 6009, Australia (e-mail: dhirendra.tripathi@research.uwa.edu.au; mariusz.martyniuk@uwa.edu.au; jarek.antoszewski@uwa.edu.au; dilusha.silva@uwa.edu.au; john.dell@uwa.edu.au; lorenzo.faraone@uwa.edu.au).

Color versions of one or more of the figures in this paper are available online at http://ieeexplore.ieee.org.

Digital Object Identifier 10.1109/JMEMS.2015.2459066

1057-7157 © 2015 IEEE. Personal use is permitted, but republication/redistribution requires IEEE permission.
See http://www.ieee.org/publications_standards/publications/rights/index.html for more information.

TABLE I
OPTICAL REFRACTIVE INDEX, n, EXTINCTION COEFFICIENT, k, QUARTER WAVE THICKNESS, t, AND ABSORPTION, a, IN A QUARTER WAVE THICK LAYER, OF VARIOUS MATERIALS AT VISIBLE (560 nm), NIR (1000 nm) AND SWIR (2000 nm) WAVELENGTHS [19]. "NGL" STANDS FOR NEGLIGIBLE

Material	560 nm				1000 nm				2000 nm			
	n	k	t (nm)	A (%)	n	k	t (nm)	A (%)	n	k	t (nm)	A (%)
Si	4.06	.038	34.8	1	3.67	4.0×10^{-4}	70	1×10^{-4}	3.45	1.5×10^{-6}	145	ngl
Ge	5.38	2.049	26.7	29	4.62	0.17	56	4	4.12	1.4×10^{-6}	122	ngl
InP	3.63	0.380	38.0	19	3.32	1.1×10^{-5}	75	5×10^{-4}	3.13	1.1×10^{-5}	160	34
GaAs	4.01	0.276	26.7	10	3.51	1.3×10^{-4}	71	ngl	3.34	1.3×10^{-4}	150	ngl
SiN_x	2.0	10^{-6}	67	ngl	1.99	10^{-6}	125	ngl	1.99	10^{-6}	250	ngl

Compound semiconductors, such as InGaN, InAlP, GaAs, AlGaInP and InP have been used extensively for realizing DBRs and filters operating from visible to short-wave infrared wavelengths (SWIR) [5]–[9] Deposition of compound semiconductors generally requires either molecular beam epitaxy (MBE) or metal organic chemical vapor deposition (MOCVD). Both these methods are high-cost processes in both set up and running costs, and tuning of the stress of these materials requires precise control of the ratio of elements in the deposited materials. Due to these issues, compound semiconductor based materials have not been adopted in mainstream MEMS manufacturing, which is based on lower-cost thin film deposition processes.

Silicon and silicon-based nitrides and oxides are widely used alternatives to compound semiconductor materials in optical MEMS technology, and are common in bulk micromachined and surface micromachined MEMS based DBRs and filters operating from SWIR wavelengths to long-wave infrared wavelengths (LWIR) [2], [5], [10]–[12].

Silicon has attractive mechanical properties, relatively inexpensive processing technologies, and availability of thin film stress tuning methods. These advantages have made silicon the mainstream MEMS material [13]–[15]. For depositing silicon based materials, many standard chemical vapor deposition (CVD) processes such as atmospheric pressure chemical vapor deposition (APCVD), low pressure chemical vapor deposition (LPCVD), plasma enhanced CVD (PECVD) and high density plasma CVD (HDPECVD) and inductively coupled plasma CVD (ICPCVD) have been used. The mechanical and optical properties of the deposited films are generally optimized using deposition parameters or subsequent annealing [16]–[19].

In order to consider the suitability of various materials for optical MEMS applications extending from visible, through the near infrared (NIR) and to the SWIR bands, it is useful to consider the data in Table I which lists the optical constants of some commonly used dielectrics for optical MEMS devices such as DBRs and filters [20]. Also shown are corresponding calculated absorption in a quarter wavelength thick optical layer for wavelengths of 560 nm, 1000 nm and 2000 nm. It is noted that SiN_x has negligible absorption at these wavelengths. However, due to its lower refractive index in comparison to other materials shown in Table I creating a high finesse FP filter using SiN_x would require a five-layer mirror stack for each of the top and bottom DBR of the filter. Although this increases the reflectivity of the mirror, it comes at the cost of reduction in the free spectral range and a more complex fabrication process [21]. InP, GaAs and Ge have high refractive indices, but their absorption in the visible wavelength range is prohibitively high. In comparison to InP, GaAs, and Ge, silicon has a relatively low extinction coefficient with a relatively high refractive index in the visible to SWIR wavelength range. By selecting a low refractive index material as the second dielectric layer for the DBRs, a large refractive index contrast between the two dielectric layers can be achieved, thus resulting in a very high finesse FP filter [21]. In this way, silicon can be used as high-index layer to fabricate FP filters operating from visible to SWIR wavelengths. However, note that the deposited silicon thin films must meet a range of criteria, including low tensile stress, low surface roughness, high refractive index, and low extinction coefficient.

ICPCVD process characteristics such as high plasma density, low electron temperature, low plasma potential, and simplicity of configuration, render ICPCVD as an ideal process for the deposition of high quality Si thin films [19]. A number of research groups have reported use of ICPCVD for optimizing the optical properties of Si in applications such as diffraction gratings and solar cells [19], [22]. Optimization of the mechanical properties of poly-silicon has been proposed for the fabrication of microphones and bimorphs [23], [24]. Silicon-based DBRs and filters raise new challenge associated with the simultaneous optimization of both optical and mechanical properties of ultra-thin silicon layers. In this paper, we report on a study to simultaneously optimize both the optical and mechanical properties of ICPCVD deposited amorphous silicon (a-Si) for optical MEMS applications.

An outstanding issue that needs to be addressed is the relationship between hydrogen concentration and the optical and mechanical properties of the CVD silicon thin films. As reported in earlier works a higher concentration of hydrogen in a-Si films leads to higher compressive stress, higher absorption coefficient, lower refractive index and higher extinction coefficient [18], [19], [25]–[29]. However, the results presented in this paper tend to dispute these previous conclusions. In particular, we will show that ICPCVD silicon thin films with the highest concentration of hydrogen can have low tensile stress, high refractive index and lower

TABLE II

SUMMARY OF PRESENTED RESULTS FOR IN-SITU OPTIMIZATION OF SILICON THIN FILMS. ALL FILMS WERE DEPOSITED AT 300 °C AND AT A 4 PASCAL DEPOSITION PRESSURE. THE FLOW RATES OF SILANE AND HELIUM WERE KEPT AT 5 sccm AND 95 sccm RESPECTIVELY

Sample	ICP Power (W)	Dep. Rate (nm/sec)	Stress (MPa)	560 nm		1000 nm		2000 nm		Hydrogen Conc. (cm^{-3})
				n	k	n	k	n	k	
1	20	7.2	200	4.91	0.456	3.91	1.4×10^{-4}	3.58	1.34×10^{-6}	1.38×10^{21}
2	26	10.6	65	4.36	0.036	3.77	3.2×10^{-4}	3.55	4.05×10^{-6}	1.18×10^{21}
3	35	11.67	-5	4.24	0.165	3.65	3.6×10^{-4}	3.51	7.61×10^{-6}	7.4×10^{20}
4	75	13.33	-85	4.23	0.128	3.6	5.0×10^{-4}	3.47	1.59×10^{-5}	6.34×10^{20}
5	150	16	-120	3.89	0.075	3.32	1.3×10^{-3}	3.36	9.4×10^{-5}	3.43×10^{20}
6	300	16.5	-550	3.44	0.051	2.95	4.1×10^{-3}	2.90	8.7×10^{-4}	3.07×10^{20}

extinction coefficient. Section II of this paper explains our experimental methods and section III will elaborate on the cause of this above mentioned apparently anomalous behavior. Section IV provides details on the optical characterization of fabricated devices, and demonstrates the effectiveness of the optimization of optical and mechanical properties of a-Si thin films for optical MEMS application.

II. EXPERIMENTAL

The deposition of a-Si thin films was performed using a SI500D ICPCVD system manufactured by SENTECH Instruments. This system uses a planar triple spiral antenna (PTSA) as the ICP source. With a 60 A current supply at a frequency of 13.56 MHz this antenna can generate an ion plasma density of 6×10^{11} cm^{-3}. The permissible deposition temperature range extends from room temperature to a maximum of 300 °C.

The investigated thin films were deposited on three substrates: (1) 320μm thick <100> oriented silicon substrates cleaved into 5 cm ×5 cm square pieces for film thickness measurements and FTIR spectroscopic analysis; (2) 70 μm thick <100> silicon wafers cleaved into 3 cm ×5 mm strips for stress characterization; and (3) 280 μm thick 1 inch × 1 inch square sapphire substrates for characterization of optical properties.

Stoney's formula was used to extract the residual stress in the silicon thin films from stress induced bowing of the substrate [30]–[32]. An in-house bench-top optical transmission measurement system was used to measure the optical transmission spectra of the layers on sapphire substrates at room temperature. This system allows single point optical measurement across a wavelength range from 550 nm to 2200 nm.

We used Cauchy's dispersion equations in the NKD Matl software to extract the refractive index and the extinction coefficient of the silicon thin films from the measured optical data. Cauchy's dispersion equations are given as:

$$n(\lambda) = n_0 + \frac{n_1}{\lambda^2} + \frac{n_2}{\lambda^4} \tag{4}$$

$$k = k_0 \exp\left(\frac{k_1}{\lambda}\right) \tag{5}$$

Where $n(\lambda)$ is the refractive index of the thin film and k is extinction coefficient of the thin film and n_0, n_1, n_2, k_0, k_1 are the coefficients for the fitting. Back-side reflections from the sapphire substrate were included in our calculations. The thickness of the deposited films was measured using a Dektak surface profiler.

Fourier Transform Infrared (FTIR) spectroscopy was carried out using a Perkin Elmer Spectrum One FTIR spectrometer. The hydrogen concentration in the silicon films was calculated using a standard method published in the literature [33], [34]. In a thin film the concentration of chemical bonds associated with oscillating species is proportional to the integrated intensity of the corresponding absorption band. In amorphous silicon the absorption peak centered around 640 cm^{-1} wavenumber corresponds to rocking mode vibrations of the silicon-hydrogen bond, whereas peaks near 2000 cm^{-1} and 2100 cm^{-1} wavenumber correspond to the stretching mode vibration of the monohydride (Si-H) and the dihydride ($Si-H_2$) bond, respectively [35]. The hydrogen bond concentration, bond concentration N_H for a single stretching mode is given by the following relationship:

$$N_H = AI = A \int \frac{\alpha(\omega)}{\omega} d\omega \tag{6}$$

where α is the absorption coefficient, ω is the angular frequency, A is a proportionality constant (oscillator strength), and I is the integrated intensity over the Gaussian fit curve of interest. The Si-H rocking mode has a peak at ~640 cm^{-1} and its bond concentration can be calculated using $N_H = A_{640}I_{640}$, with oscillator strength A_{640} of 1.6×10^{19} cm^{-2}. The total hydrogen concentration measured by the integrated intensity of the peak at ~640 cm^{-1} wavenumber, is the best measure of hydrogen concentration, since other peaks are less reliable [36]–[38]. Therefore, in this work, the peak at ~640 cm^{-1} wavenumber has been used to calculate hydrogen concentration. However, other peaks at 2100 cm^{-1} and 2000 cm^{-1} wavenumber are used to extract vital bonding information regarding the nature of silicon-hydrogen bonding in the amorphous silicon thin film.

The description and title of Table II lists all ICPCVD process parameters used to deposit the silicon thin films. Flow rates of silane and helium were selected based on the manufacturer recommendations of using 5 % diluted process gases for optimal quality films. The chamber pressure was fixed at 4 Pa after a separate experiment indicated that higher pressures led to an unstable plasma and the formation of polysilane powder on the films, which has been reported previously for PECVD reactors in certain pressure ranges [39], [40].

For samples 1 - 6, the ICP power was varied, deposition temperature, deposition pressure, He and SiH_4 gases flow

were kept constant at 300 °C, 4 Pa, 5 sccm and 95 sccm, respectively. All samples were tested for chemical stability against common chemicals used in microfabrication, such as photoresist developers and HF.

III. Effect of ICP Power Variations

As shown in Table II, in order to study the effect of ICP power on the quality of deposited a-Si thin films, the ICP power was varied from 20 W to 300 W while all other process parameters were kept unchanged. As evident from Table II, a positive correlation was evident between the deposition rate and ICP power. In the low ICP power range (below 50 W) the deposition rate increases rapidly with increasing ICP power, and eventually saturates in the high ICP power range (above 150 W) [41]. Films deposited in the ICP power range of 20 W to 25 W were found to be tensile. The value of the residual tensile stress was found to decrease with increasing ICP power, eventually crossing over to compressive residual stress values near an ICP power value of 35 W. Any further increase in ICP power results in increasing values of compressive stress, with a-Si films deposited at 300 W exhibiting 550 MPa of compressive residual stress. Earlier work by our research group had found that the average Young's modulus for as deposited ICPCVD a-Si thin films range from 120 GPa to 133 GPa. The average hardness for the as deposited a-Si ranged from 9.5 GPa to 10.3 GPa. A part of the research work is published in Ref. [42].

Figure 1(a) shows the measured transmittance from 550 nm-2250 nm as a function of ICP power. The number of interference fringes does not change with variations in the ICP power. However their position and magnitude of maxima and minima varies with the ICP power. Since the thickness of all the films was ∼500 nm, the variation in position of maxima and minima indicates that there is change of refractive index with a variation in ICP power. The longer the wavelength at which the maxima occur, the higher will be the refractive index. Thus, the ICP power lower than 75 W should produce high refractive index films, which was later confirmed by the extraction of optical constants. In the visible wavelength region (550-700 nm), for the ICP powers of 75 W and less, we see a sharp decay in the magnitude of the interference curve. This indicates that this region is having higher absorption than in the NIR and SWIR wavelength region (700-2250 nm). This was later confirmed from the higher extinction coefficient found in this wavelength range. In the short wavelength region the absorption of the Si films with the ICP power 75 W and lower is less hence we see a large increase in transmittance. The transmittance pattern of Si films deposited at 150 W and 300 W ICP power shows a lower magnitude in comparisons to transmittance of the films deposited at 75 W or lower ICP power. This indicates a higher absorption in films deposited at 150 W and 300 W in the SWIR wavelength region, as compared to the films deposited at 75 W or lower ICP power. The detailed theory of interference patterns and their relationship with optical constant can be found in Ref. [43]. The rms roughness of all the films was measured with a Vecco dimension 3000 AFM and it lies within the range of 1-4 nm. with such low value of roughness we don't expect any effect on the interference pattern and optical properties of silicon films.

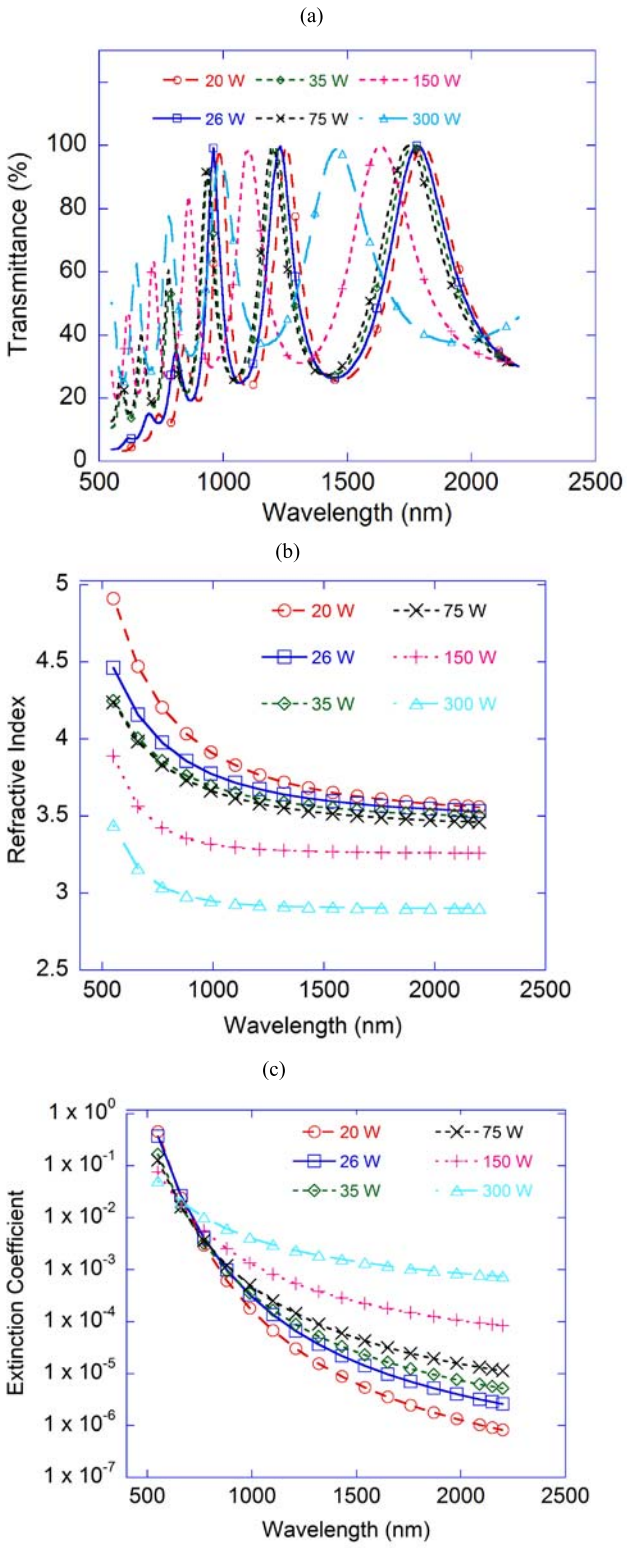

Fig. 1. (a) Measured optical transmittance spectra as a function of ICP power; (b) Refractive index for various of ICP powers; (c) Extinction coefficient for various ICP powers.

Figure 1(b) and (c) show the measured optical constants of the individual samples as a function of wavelength for

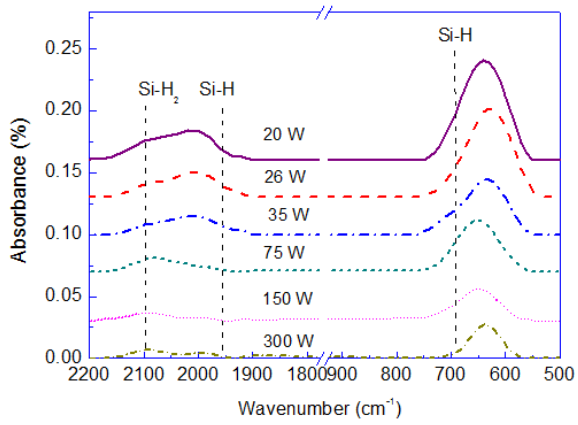

Fig. 2. FTIR spectra of the ICPCVD Si films deposited at 300 °C using various ICP powers.

films deposited using various ICP powers. It is evident from Fig. 1(b) that with a decrease in ICP power the refractive index increases for all samples regardless of wavelength range. In Fig. 1(c) the extinction coefficient is well-correlated with ICP power, with a negative correlation at visible wavelengths (500-700 nm), and a positive correlation at SWIR wavelengths (1500-2250 nm). The crossover in this correlation occurs near a wavelength of 700 nm. At visible wavelengths (500-700 nm) the relatively high extinction coefficient (0.012–0.456) of the films would generally be considered to be detrimental for realization of FP filters. However, this effect, is somewhat alleviated since films required for this wavelength range are very thin (less than 100 nm thick), hence the total absorption through the filters and DBRs can be kept low. Thus, filters and DBRs fabricated with such thin films should still produce adequate optical performance at visible wavelengths.

Figure 2 shows measured FTIR spectra for thin film samples no. 1 to 6 that were deposited with ICP power varying from 20 W to 300 W. The spectra have been offset for clarity. Note that with increasing ICP power the absorbance due to the hydrogen bonds decreases, both for the rocking vibration mode (640 cm^{-1}) and the stretching vibration mode (2000-2200 cm^{-1}).

At 75 W ICP power the Si-H_2 stretching bond peak at (2100 cm^{-1}) dominates over the monohydride stretching mode vibration peak. For ICP power of 150 W and 300 W, we note the simultaneous presence of Si-H and Si-H_2 peaks. We also observed that for a variation in ICP power the FWHM of peaks at ∼640 cm^{-1} is constant and equal to 100 cm^{-1}. Generally, the variation in FWHM of FTIR spectra is considered as indicator of variation in the stoichiometry of the PECVD deposited materials [44]. Thus, the observed constant FWHM in the ICPCVD deposited amorphous silicon indicates a constant stoichiometry for these films.

The data reported in Fig. 2 has been used to estimate the hydrogen concentration in the films, which is shown in the last column of Table II as a function of ICP power. As ICP power increases, the hydrogen concentration in the films is significantly reduced. This is an interesting observation to note. In previous studies a higher hydrogen concentration in CVD silicon thin films has generally been associated with more compressive films, which has been shown to have a detrimental effect on the optical properties [18]. However, as noted previously in this section, we have observed that an increase in hydrogen concentration is directly correlated with a decrease in ICP power, results in improved optical quality of the films (see Fig.1), and renders films more tensile (see Table II). This apparent contradiction can be explained by careful consideration of the physical mechanisms whereby hydrogen is incorporated into the amorphous silicon films.

In the ICP plasma a variety of neutral radicals, ionic and emissive species are generated by the ionization of SiH_4. The neutral radicals SiH_2 and SiH_3 are the dominant contributors to film growth and, since the SiH_3 radical has the longest life time, it is considered to be the major contributor to growth of the film [35], [45]. The sticking coefficient of neutral SiH_3 radicals to the surface of the growing film is a critical parameter, which depends on the available locations and the deposition temperature.

The density of ionic species such as H^+, H_2^+, SiH_x^+ and $Si_2H_y^+$ on the growing surface is significantly lower in comparison to neutral radicals and, thus, their contribution to the deposition rate can be neglected. However, their higher kinetic energy in comparison to neutral ions results in a significant impact on the properties of the film. Matsuda and Tanaka [41] reported that impinging ionic species on the growing surface gives rise to compressive stress in films.

As shown in Table II the deposition rate at 20 W is only 7.2 nm/sec. Due to the low ICP power, the density of neutral and ionic species is low, leading to a low growth rate. The low density of neutral radicals, combined with a high deposition temperature (300 °C), assists neutral radicals such as SiH_3 to diffuse over a longer distance and thus form a denser network of strong Si-Si and Si-H bonds. Under these conditions, the dangling bond density is low and it is plausible that most of the hydrogen tied up in the passivation of dangling bonds ends up forming stable Si-H bonds. Thus, for the films deposited at 20 W, the FTIR spectrum in Fig. 2 shows the highest absorption for the Si-H rocking bond at 640 cm^{-1} wavenumber. As a result of forming stable Si-H bonds, our results indicate that, despite having the highest hydrogen concentration, films deposited at 20 W ICP power have the highest refractive index (see Fig. 2(a)) and the highest value of tensile stress among all deposited films (see Table II).

As the ICP power is increased, the density of neutral and ionic species in the plasma also increases, which increases the growth rate of the film. However, it also reduces the diffusion length of neutral radicals. Therefore, many dangling bonds in the growing film remain unpassivated, which leads to an increase in the defect density within the film. The increased defect density, in turn, results in a decrease in the refractive index with increasing ICP power. The increase in defect density with increase in ICP power also leads to higher absorption in the SWIR wavelength range (1500-2250∼nm). The increase in ICP power also increases the optical band gap of amorphous silicon, which decreases absorption in the visible wavelength range (500-700 nm) [46], [47] (see Fig. 1(b)). Eventually at 150 W and 300 W ICP power we see saturation

TABLE III
SUMMARY RESULTS OF FABRICATED DBRS

Class of DBR operation	Wavelength Range (nm)	Thickness of layer 1 (Si) (nm)	Thickness of layer 2 (SiO_x) (nm)	Thickness of layer 3 (Si) (nm)	Measured peak reflectivity (%)	Simulated Peak reflectivity (%)	Measured Fractional bandwidth ($\Delta\lambda/\lambda$) (%)
VIS	500–700	41	100	36	88	93	33.3
NIR	710–1000	60	132	62	89	92	36.25
SWIR	2040–3040	185	400	190	86	90	41.67

of deposition rate which indicates an equilibrium condition where the deposition rate is solely governed by sticking of neutral radicals on the available locations [41].

With a continued increase in ICP power, the density of ionic species also continues to increase. Initially, this reduces the tensile stress until, finally, at an ICP power of 35∼W and above, the stress in the films eventually becomes compressive. With further increase in ICP power the compressive stress increases, which is in agreement with the findings of Matsuda *et al.* [41].

However, our results contradict the results reported in Refs [28], [29], where the authors suggest that a higher hydrogen concentration is the sole factor leading to a lower refractive index and higher compressive stress in their silicon films. From our experimental observations, we propose that if hydrogen in the film forms a stable bond with silicon, then even a relatively high concentration of hydrogen can lead to a dense and tensile film.

A summary of the results for the presented optimization process are shown in Table II.

IV. EXPERIMENTAL RESULTS FOR VISIBLE, NIR AND SWIR WAVELENGTH DBRS AND SUSPENDED MEMBRANE STRUCTURES

In order to confirm the optical performance of the ICPCVD silicon thin films, we fabricated Si-SiO_x-Si tri-layer based DBRs for the SWIR, NIR and visible bands on 310 μm thick sapphire substrates. The measured refractive index of ICPCVD deposited SiO_x layers, at a wavelength of 632 nm was 1.45. This is equivalent to 1.46, the refractive index of stoichiometric silicon dioxide (SiO_2) at the same wavelength [20]. Hence, we expect the stoichiometric factor x in SiO_x is close to 2. The ICPCVD deposited SiO_x layers show negligible extinction coefficient in the visible to SWIR wavelength range. Each layer was a quarter wavelength thick at the center-wavelength of the appropriate band. Since the optical properties of silicon oxide are well-known, these DBRs can be used to confirm the optical properties of the silicon for optical MEMS applications. Based on the deposition rate, low tensile stress, and adequate optical constants, the silicon recipe chosen for DBR fabrication was that of sample 2 in Table II. The silicon oxide deposition parameters were ICP power – 450 W, deposition pressure – 4 Pa, deposition temperature -130 °C, SiH_4, N_2O, He and Ar flow rates- 6.5 sccm, 70 sccm, 123 sccm and 120 sccm, respectively. Table III lists the measured thicknesses of the constituent layers, the measured and simulated peak reflectivity, and the corresponding fractional optical bandwidth ($\Delta\lambda/\lambda$).

Figure 3 shows the measured and simulated reflectance spectra of the DBRs. Simulation of the optical properties of DBRs was undertaken using the optical matrix transmission method [21] taking the measured optical constants and thicknesses of deposited silicon and silicon oxide layers as input to the model. The measured peak reflectivity for the DBRs fabricated using the ICPCVD silicon films reach 88-89 %, which is close to the theoretically predicted value of 92-93 %. There is a 3-5% variation between the simulated and measured reflectivity, which can be attributed to two possible reasons. The first is a small variation in the properties of materials deposited in the ICPCVD reactor from run to run causing the properties to change slightly. Another possibility is that the simulations use optical constants of amorphous silicon films which were ∼500 nm thick. We expect like any other PECVD material optical constants may show a slight variation based on thickness of the films. However, a detailed study of how thickness affects the optical properties of amorphous silicon films will be the subject of a future study.

One of the most important points to note from Fig. 3(a) and (b) is the close to 90 % reflectance of the DBRs operating in the visible spectrum (500-650 nm) and near infrared spectrum (700-1000 nm). This validates our previous comment that despite significant absorption at visible and near infrared wavelengths, the thin quarter wavelength layers of silicon result in high-reflectivity DBRs and are suitable for FP filter fabrication. These mirrors have been shown to exhibit a large fractional optical bandwidth, which render them suitable for applications such as spectroscopy over a relatively broad spectral range.

The influence of the stress optimization process was evaluated by freely suspending a 141 nm thick silicon layer over a 270 μm diameter circular pattern supported only at its periphery. A silicon thickness of 141 nm was chosen because this corresponds to a quarter-wave thickness at a wavelength of 2000 nm. The silicon recipe used for deposition was the same as that used for fabricating the above-mentioned DBRs. As discussed previously, this recipe results in 65∼MPa of tensile stress. Hence, a flat suspended structure is expected, which can be used for the fabrication of a high finesse FP cavity.

The fabrication process was carried out on 300 μm thick <100> oriented silicon substrates. The Following fabrication process flow was used for the suspended membrane structure:

1. 20 % diluted PI2610 polyimide was spun, soft-baked at 100 °C for five minutes and hard-baked at 300 °C for 20 minutes.

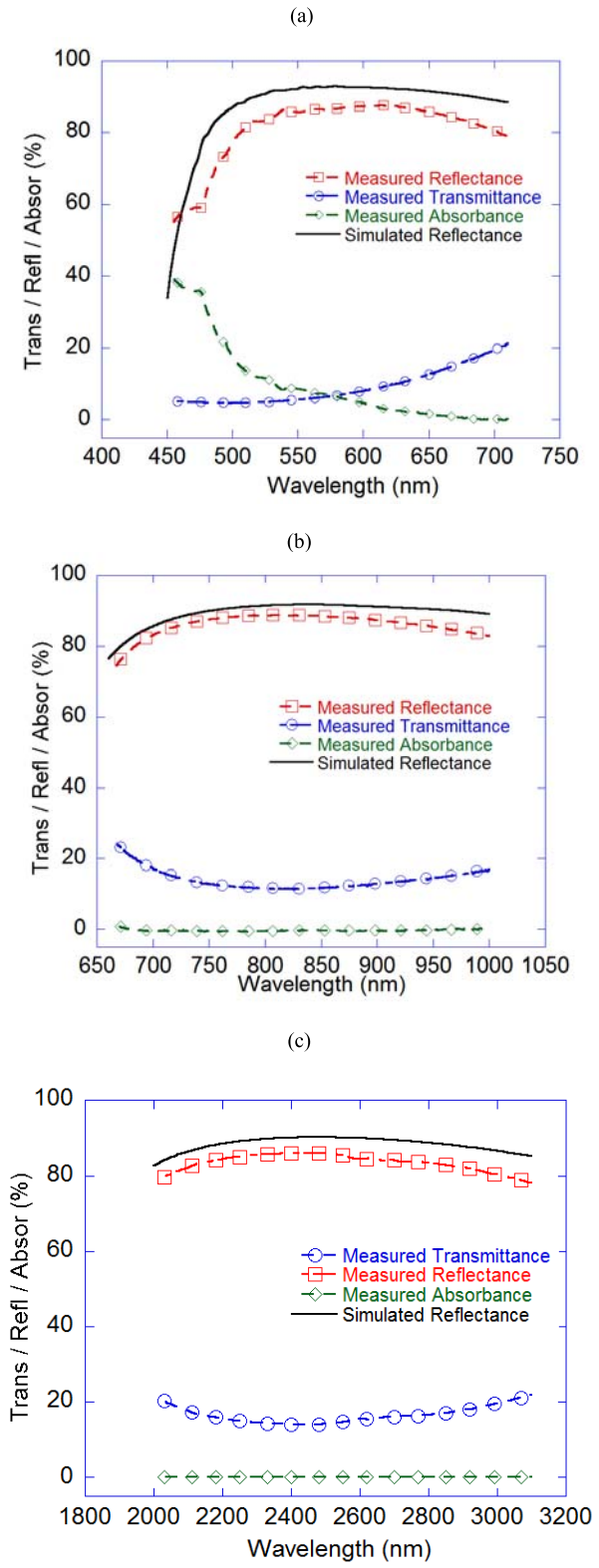

Fig. 3. Measured transmittance, reflectance and absorbance of fabricated three layer silicon-silicon oxide-silicon DBRs. The solid lines represent the simulated reflectance for each DBR for comparison with the measured reflectance data (a) visible wavelength DBR, (b) NIR wavelength DBR, (c) SWIR wavelength DBR.

2. The 300 nm thick polyimide was patterned in an O_2/CF_4 plasma at room temperature, which served as the sacrificial layer. The etch recipe for polyimide was: RF power- 26 W, pressure- 2.67 Pa, O_2/CF_4 flow rate- 30/3 sccm.
3. Subsequently, the 141nm thick silicon layer was deposited, and 5μm diameter etch holes were perforated into the silicon film using a CF_4 based plasma recipe, RF power-100 W, ICP power- 400 W pressure- 4 Pa, CF_4 flow rate- 30 sccm. The etch holes are spaced 50 um apart, and separate experiments have shown that this sparse density of holes does not affect the resultant film stress.

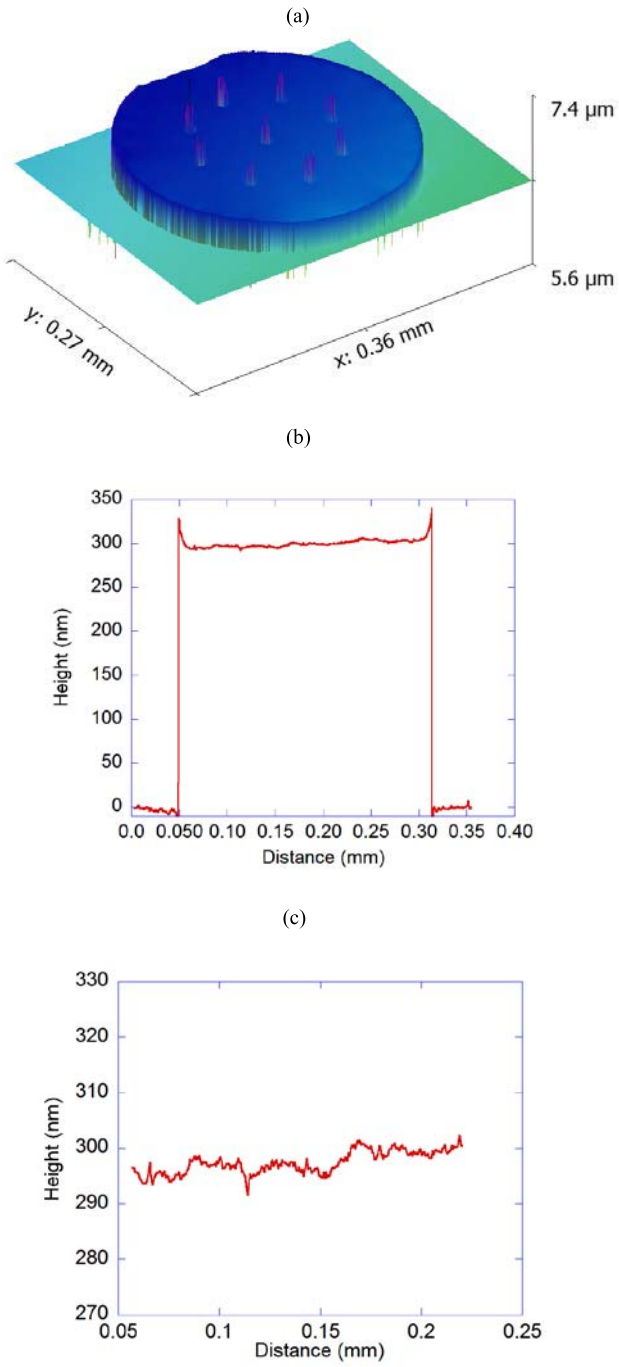

Fig. 4. Optical surface profiles of fabricated 270 μm diameter circular structure, (a) 3-D surface profile, (b) extracted line scan across the suspending membrane avoiding the etch holes, and (c) profile of fabricated structure on an expanded vertical scale.

4. The sacrificial layer was then etched in a barrel asher in an oxygen plasma to release the 141 nm thick silicon membrane, thus yielding a final suspended structure.

Figure 4(a) shows the 3-D optical profile of the suspended structure, obtained using a Zygo surface profiler, and Fig. 4(b) shows a cross section of the suspended film. The sharp peaks, in Fig. 4(b) at the either ends across the 270 μm diameter suspended structure, are due to the limitation of optical measurement over the sharp edges. In Fig. 4(c), which is an expanded scale plot of Fig. 4(b), it is noted that the suspended film shows exceptional surface flatness, with a variation on the order of 6$\sim$nm across the structures diameter.

V. Conclusion

This paper describes optimization of the optical properties and stress in ICPCVD amorphous silicon thin films. Our previous work has demonstrated suitable mechanical properties for MEMS applications. The optimized amorphous silicon films can be used to fabricate high performance optical MEMS devices operating from the visible, through NIR to the SWIR wavelengths. Optimisation of the thin film properties has been investigated as a function of the magnitude of ICP power during deposition. We have showed a strong correlation between decreasing ICP power and increasing refractive index of the amorphous silicon films, regardless of the wavelength range. The extinction coefficient showed a negative correlation with ICP power for visible wavelengths, and a positive correlation with ICP power for SWIR wavelengths. In particular, it has been shown that high quality films for optical MEMS applications can be obtained despite the incorporation of a significant concentration of hydrogen. We conclude that the presence of hydrogen actually assists in the formation of stable and strong Si-H bonds, thus reducing the defect density in the films and improving their optical quality. As a demonstration vehicle, DBRs operating from visible to SWIR wavelength range were fabricated, with close to 90 % measured peak reflectivity. Furthermore, a controllable level of tensile stress was verified via fabrication of an ultraflat suspended silicon film. The flatness measurement over a lateral dimension of 270 μm, avoiding the etch holes, shows variation on the order of 6 nm.

Acknowledgment

This work was performed in part at the Western Australian node of the Australian National Fabrication Facility, a company established under the National Collaborative Research Infrastructure Strategy to provide nano and micro-fabrication facilities for Australian researchers. The authors also acknowledge support from the Western Australian State government Office of Science.

References

[1] R. F. Wolffenbuttel, "MEMS-based optical mini- and microspectrometers for the visible and infrared spectral range," *J. Micromech. Microeng.*, vol. 15, no. 7, pp. S145–S152, 2005.

[2] A. Lipson and E. M. Yeatman, "A 1-D photonic band gap tunable optical filter in (110) silicon," *J. Micromech. Syst.*, vol. 16, no. 3, pp. 521–527, Jun. 2007.

[3] R. A. Crocombe, "Miniature optical spectrometers: There's plenty of room at the bottom part I, Background and mid-infrared spectrometers," *Spectroscopy*, vol. 23, no. 1, p. 38, 2008.

[4] E. Garmire, "Theory of quarter-wave-stack dielectric mirrors used in a thin Fabry–Perot filter," *Appl. Opt.*, vol. 42, no. 27, pp. 5442–5449, 2003.

[5] J. H. Jerman, D. J. Clift, and S. R. Mallinson, "A miniature Fabry–Perot interferometer with a corrugated silicon diaphragm support," presented at the IEEE Solid-State Sensor and Actuator Workshop, Jun. 1990.

[6] N. Chitica, J. Daleiden, M. Strassner, and K. Streubel, "Monolithic InP-biased tunable filter with 10-nm bandwidth for optical data interconnects in the 1550-nm band," *IEEE Photon. Technol. Lett.*, vol. 11, no. 5, pp. 584–586, May 1999.

[7] F. Riemenschneider, M. Aziz, H. Halbritter, I. Sagnes, and P. Meissner, "Low-cost electrothermally tunable optical microcavities based on GaAs," *IEEE Photon. Technol. Lett.*, vol. 14, no. 11, pp. 1566–1568, Nov. 2002.

[8] M. Garrigues, J. Danglot, J.-L. Leclercq, and O. Parillaud, "Tunable high-finesse InP/air MOEMS filter," *IEEE Photon. Technol. Lett.*, vol. 17, no. 7, pp. 1471–1473, Jul. 2005.

[9] N. Nakada, M. Nakaji, H. Ishikawa, T. Egawa, M. Umeno, and T. Jimbo, "Improved characteristics of InGaN multiple-quantum-well light-emitting diode by GaN/AlGaN distributed Bragg reflector grown on sapphire," *Appl. Phys. Lett.*, vol. 76, no. 14, pp. 1804–1806, 2000.

[10] S. Irmer *et al.*, "Surface micromachined optical low-cost all-air-gap filters based on stress-optimized Si_3N_4 layers," *J. Micromech. Microeng.*, vol. 15, no. 4, pp. 867–872, 2005.

[11] B. Saadany, M. Malak, F. Marty, Y. Mita, D. Khalil, and T. Bourouina, "Electrostatically-tuned optical filter based on silicon Bragg reflectors," presented at the IEEE/LEOS International Conference on Optical MEMS and their Applications Conference, Aug. 2006.

[12] M. Tuohiniemi and M. Blomberg, "Surface-micromachined silicon air-gap Bragg reflector for thermal infrared," *J. Micromech. Microeng.*, vol. 21, no. 7, p. 075014, 2011.

[13] K. E. Petersen, "Silicon as a mechanical material," *Proc. IEEE*, vol. 70, no. 5, pp. 420–457, May 1982.

[14] W. P. Eaton and J. H. Smith, "Micromachined pressure sensors: Review and recent developments," *Smart Mater. Struct.*, vol. 6, no. 5, pp. 530–539, 1997.

[15] G. T. A. Kovacs, I. N. Maluf, and K. E. Petersen, "Bulk micromachining of silicon," *Proc. IEEE*, vol. 86, no. 8, pp. 1536–1551, Aug. 1998.

[16] M. Janai, D. D. Allred, D. C. Booth, and B. O. Seraphin, "Optical properties and structure of amorphous silicon films prepared by CVD," *Solar Energy Mater.*, vol. 1, pp. 11–27, Feb. 1979.

[17] A. Pleschinger, J. Lutz, F. Kuchar, H. Noll, and M. Pippan, "Study of polycrystalline and amorphous LPCVD silicon films by atomic force microscopy," *Surf. Interf. Anal.*, vol. 25, pp. 529–532, Jun. 1997.

[18] W.-C. Hsiao, C.-P. Liu, and Y.-L. Wang, "Influence of RF bias on hydrogenated amorphous silicon by high-density plasma chemical vapor deposition," *J. Electrochem. Soc.*, vol. 154, no. 5, pp. G122–G126, 2007.

[19] Y. Qin, H. Yan, F. Li, L. Qiao, Q. Liu, and D. He, "The optoelectronic properties of silicon films deposited by inductively coupled plasma CVD," *Appl. Surf. Sci.*, vol. 257, no. 3, pp. 817–822, 2010.

[20] E. D. Palik, *Handbook of Optical Constants of Solids*. San Diego, CA, USA: Academic, 1998.

[21] H. A. Macleod, *Thin-Film Optical Filters*. New York, NY, USA: McGraw-Hill, 1989.

[22] W.-J. Liu, S. Chen, H.-Y. Cheng, J.-D. Lin, and S.-L. Fu, "Fabrication of amorphous silicon films for arrayed waveguide grating application," *Surf. Coat. Technol.*, vol. 201, no. 15, pp. 6581–6584, 2007.

[23] S. Chang and S. Sivoththaman, "Development of a low temperature MEMS process with a PECVD amorphous silicon structural layer," *J. Micromech. Microeng.*, vol. 16, no. 7, pp. 1307–1313, 2006.

[24] A. Torkkeli, O. Rusanen, J. Saarilahti, J. Hietanen, H. Seppä, and H. Sipola, "Capacitive microphone with low-stress polysilicon membrane and high-stress polysilicon backplate," *Sens. Actuators A, Phys.*, vol. 85, pp. 116–123, Aug. 2000.

[25] H.-J. Lin and S.-H. Chen, "Effect of the hydrogen concentration on the growth mechanism of sputtered hydrogenated silicon thin films," *Opt. Mater. Exp.*, vol. 3, no. 9, pp. 1215–1222, 2013.

[26] J. Gope, S. Kumar, A. Parashar, S. Dayal, C. M. S. Rauthan, and P. C. Srivastava, "Effect of hydrogen content and bonding environment on mechanical properties of hydrogenated silicon films deposited by high-frequency PECVD process," *ISRN Nanomater.*, vol. 2012, May 2012, Art. ID 429348.

[27] M. Wu, W. Li, Y. Qiu, J. Fu, and Y. Jiang, "Hydrogen bonding in hydrogenated amorphous silicon thin films prepared at different precursor gas temperatures with undiluted silane," *Sci. China Technol. Sci.*, vol. 54, no. 9, pp. 2310–2314, 2011.
[28] F. Gaspari, "Optoelectronic properties of amorphous silicon the role of hydrogen: From experiment to modeling," in *Optoelectronics-Materials and Techniques*. Rijeka, Croatia: InTech, 2011.
[29] H. Kakinuma, S. Nishikawa, T. Watanabe, and K. Nihei, "Intrinsic stress and hydrogen bonding in glow-discharge amorphous silicon films," *J. Appl. Phys.*, vol. 59, no. 9, p. 3110, 1986.
[30] G. G. Stoney, "The tension of metallic films deposited by electrolysis," *Proc. Roy. Soc. London A*, vol. 82, pp. 172–175, May 1909.
[31] H. Guckel, D. Burns, C. Rutigliano, E. Lovell, and B. Choi, "Diagnostic microstructures for the measurement of intrinsic strain in thin films," *J. Micromech. Microeng.*, vol. 2, no. 2, pp. 86–95, 1992.
[32] X. Feng, Y. Huang, and A. J. Rosakis, "On the Stoney formula for a thin film/substrate system with nonuniform substrate thickness," *J. Appl. Mech.*, vol. 74, no. 6, pp. 1276–1281, 2007.
[33] D. K. Basa and F. W. Smith, "Annealing and crystallization process in a hydrogenated amorphous Si–C alloy film," *Thin Solid Films*, vol. 192, no. 1, pp. 121–133, 1990.
[34] L.-W. Lai, H.-Y. Lee, J.-H. Cheng, and C.-T. Lee, "Investigation of laser-assisted microcrystalline SiGe films deposited at low temperature," *J. Electron. Mater.*, vol. 37, no. 2, pp. 167–171, 2008.
[35] R. A. Street, *Hydrogenated Amorphous Silicon*. Cambridge, U.K.: Cambridge Univ. Press, 1991.
[36] E. Bustarret, M. Bensouda, M. C. Habrard, J. C. Bruyère, S. Poulin, and S. C. Gujrathi, "Configurational statistics in a-$Si_xN_yH_z$ alloys: A quantitative bonding analysis," *Phys. Rev. B*, vol. 38, no. 12, pp. 8171–8184, 1988.
[37] A. A. Langford, M. L. Fleet, B. P. Nelson, W.A. Lanford, and N. Maley, "Infrared absorption strength and hydrogen content of hydrogenated amorphous silicon," *Phys. Rev. B*, vol. 45, p. 13367, Jun. 1992.
[38] H. Shanks, C. J. Fang, L. Ley, M. Cardona, F. J. Demond, and S. Kalbitzer, "Infrared spectrum and structure of hydrogenated amorphous silicon," *Phys. Status Solidi B*, vol. 100, no. 1, pp. 43–56, 1980.
[39] G. Oversluizen and W. H. M. Lodders, "Optimization of plasma-enhanced chemical vapor deposition of hydrogenated amorphous silicon," *J. Appl. Phys.*, vol. 83, no. 12, pp. 8002–8009, 1998.
[40] W. H. M. Lodders, "Powder formation in silane plasma's," Philips Res. Lab., Tech. Rep., 1997.
[41] A. Matsuda and K. Tanaka, "Investigation of the growth kinetics of glow-discharge hydrogenated amorphous silicon using a radical separation technique," *J. Appl. Phys.*, vol. 60, no. 7, pp. 2351–2356, 1986.
[42] K. L. Brookshire, M. Martyniuk, K. K. M. B. D. Silva, Y. Liu, and L. Faraone, "Long-term stability of ICPCVD a-Si under prolonged heat treatment," in *Proc. Conf. Optoelectron. Microelectron. Mater. Devices (COMMAD)*, Perth, WA, USA, 2014, pp. 160–163.
[43] R. Swanepoel, "Determination of the thickness and optical constants of amorphous silicon," *J. Phys. E, Sci. Instrum.*, vol. 16, no. 12, pp. 1214–1222, 1983.
[44] G. Lucovsky, M. J. Manitini, J. K. Srivastava, and E. A. Irene, "Low-temperature growth of silicon dioxide films: A study of chemical bonding by ellipsometry and infrared spectroscopy," *J. Vac. Sci. Technol. B*, vol. 5, no. 2, pp. 530–537, 1987.
[45] F. J. Kampas and R. W. Griffith, "Origin of emitting species in the plasma deposition of a-Si:H alloys," *J. Appl. Phys.*, vol. 52, no. 3, p. 1285, 1981.
[46] A. Nakajima, Y. Sugita, K. Kawamura, H. Tomita, and N. Yokoyama, "Microstructure and optical absorption properties of Si nanocrystals fabricated with low-pressure chemical-vapor deposition," *J. Appl. Phys.*, vol. 80, no. 7, pp. 4006–4011, 1996.
[47] A. Shyam, "Fabrication of high quality, low bandgap amorphous silicon & amorphous silicon Germanium alloy solar cell by chemical annealing," Ph.D. dissertation, School Elect. Eng., Iowa State Univ., Ames, IA, USA, 2011.
[48] J. Daleiden *et al.*, "Tunable InP/Air gap Fabry Perot filter for wavelength division multiplex fiber optical transmission," presented at the 11th International Conference on Indium Phosphide and Related Materials, Davos, The Switzerland, 1999.

Dhirendra Kumar Tripathi received the B.Tech. degree in electronics engineering from UPTU University, Lucknow, in 2005, and the M.Tech. degree in VLSI systems from NIT, Trichy, India, in 2008. He is currently pursuing the Ph.D. degree with the School of Electrical, Electronic, and Computer Engineering, University of Western Australia, Crawley Perth, Australia. His current research activities involve the design and fabrication of optical MEMS devices and materials for the MEMS.

Fei Jiang was born in China, in 1983. He received the B.E. and M.A. degrees in materials science from the Harbin University of Science and Technology, Harbin, China, in 2005 and 2008, respectively, and the Ph.D. degree in electrical and electronic engineering and mechanical engineering from the University of Western Australia (UWA), Crawley, Australia, in 2008.

He was a Graduate Research Assistant with UWA. He is currently with MRX Technologies. His research activities are in the fields of microelectromechanical systems (MEMS) actuators and optical MEMS spectrometers.

Mariusz Martyniuk was born in Poland, in 1976. He received the B.Sc. (Hons.) degree from the University of Toronto, ON, Canada; the M.A.Sc. degree from McMaster University, ON; and the Ph.D. degree in 2007 from the University of Western Australia, Perth, Australia.

He worked in the industry sector as an Electronics Engineer. He joined the University of Western Australia, where he is currently a Research Professor with the Microelectronics Research Group and manages the Western Australian Node of the Australian National Fabrication Facility. His primary areas of interest encompass thin-film materials and thin-film mechanics, and their applications in microelectromechanical systems and optoelectronic devices.

Dr. Martyniuk's research contributions were recognized in 2008 by the award of the inaugural Australian Museum Eureka Prize (the Oscars of Australian science) for the Outstanding Science in support of Defense or National Security.

Jarek Antoszewski received the Master's degree in physics from the Teachers College, Olsztyn, Olsztyn, Poland, in 1977, and the Ph.D. degree in semiconductor physics from the Institute of Physics, Polish Academy of Science, Warsaw, Poland, in 1982. From 1982 to 1990, he was a Researcher and a Project Leader with the Research and Development Laboratory, WILMER Ltd., Warsaw, where he was involved in the design and testing of infrared radiometers for industrial applications. In 1991, he joined the Microelectronics Research Group, University of Western Australia, Crawley, W.A., Australia, where he has been involved in magneto-transport studies of semiconductor materials, and physics and technology of infrared detectors. His current research interests include development of technology merging II–VI and III–V-based infrared detectors with microelectromechanical technology into a new technology for monolithic tunable infrared sensors.

K. K. M. B. Dilusha Silva was born in Sri Lanka, in 1973. He received the (Hons.) degrees in physics and electronic engineering from the University of Western Australia (UWA). His Ph.D. was awarded in 2004 after completing research in optical imaging technologies for biomedical applications. He has worked both in industry and academia, and currently holds the positions of Research Professor and Engineering Manager at the Microelectronics Research Group at UWA. Since returning to UWA in 2009, his research interests include optical microelectromechanical systems (MEMS) sensors, optical spectroscopic sensors, and MEMS biosensors. He has attracted funding for his research from the agriculture, aerospace, and government, and is leading a number of MEMS related research efforts at MRG with strong commercial links into both the agricultural and aerospace sectors.

John M. Dell is currently a Professor of Electrical Engineering with the University of Western Australia, Perth, Australia.

His primary areas of interest are semiconductor optoelectronics and optical MEMS devices. He has worked in both industry and academia in these fields.

He has several patents, a over 200 and journal and conference publications. Work undertaken by his group on robust low-cost microspectrometer technology has attracted funding from the U.S. and Australian Defense Departments, and more recently, from the Australian Grains Research and Development Corporation. This latter funding is for the development of low-cost tools using IR spectroscopy for broad acre agriculture applications. This work is being undertaken as a collaboration between electrical engineers and soil scientists.

Lorenzo Faraone was born in Italy, in 1951. He received the Ph.D. degree from the University of Western Australia (UWA), Perth, Australia, in 1979.

He was a Research Scientist with Lehigh University, PA, (1979-1980), where he was involved in studies on MOS devices. From 1980 to 1986, he was a Member of the Technical Staff with RCA Laboratories, David Sarnoff Research Center, Princeton, NJ, where he was involved in VLSI CMOS and nonvolatile memory technologies, and space radiation effects in silicon-on-sapphire MOS integrated circuits. He joined the School of Electrical, Electronic, and Computer Engineering at UWA, in 1987, where he has held the position of Professor since 1998, and the position of Head of the Department/School from 1999 to 2003. Since his arrival at UWA, his research interests have been in the area of compound semiconductor materials and devices, and microelectromechanical systems (MEMS). In particular, his interests include Mercury Cadmium Telluride materials and device technologies for infrared detector arrays, Gallium Nitride technology for ultraviolet detectors and high-speed/high-power electronics, and MEMS technologies for tuneable optical cavity infrared detectors. He currently holds more than ten U.S. patents, has supervised more than 25 Ph.D. student completions, and has authored over 300 refereed technical papers in journals and conference proceedings.

Prof. Faraone received the RCA Laboratories Individual Outstanding Achievement Award in 1983 and 1986, and the John de Laeter Innovation Award in 1997.